Genetic Algorithm-Based Fuzzy Controller for Improving the Dynamic Performance of Self-Excited Induction Generator

Abdel-Fattah Attia, Yusuf. A. Al-Turki & Hussein F. Soliman

Arabian Journal for Science and Engineering

ISSN 1319-8025

Arab J Sci Eng
DOI 10.1007/s13369-012-0211-8

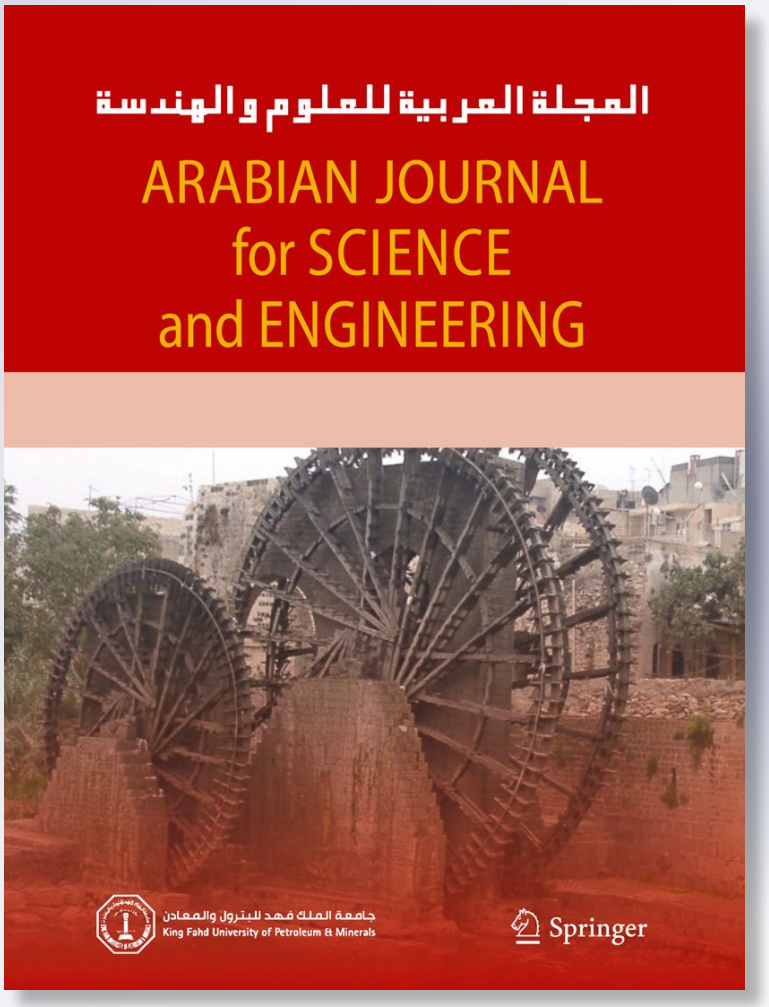

Springer

Arab J Sci Eng
DOI 10.1007/s13369-012-0211-8

RESEARCH ARTICLE - ELECTRICAL ENGINEERING

Abdel-Fattah Attia · Yusuf. A. Al-Turki · Hussein F. Soliman

Genetic Algorithm-Based Fuzzy Controller for Improving the Dynamic Performance of Self-Excited Induction Generator

Received: 15 June 2010 / Accepted: 25 December 2010

Abstract This paper introduces a new hybrid controller using artificial intelligence (AI) techniques to improve the dynamic performance of the self-excited induction generator "SEIG" driven by wind energy conversion scheme "WECS". The hybrid AI compromises a genetic algorithm (GA) and fuzzy logic controller (FLC). The role of the GA is to optimize the parameters of the fuzzy set to ensure a better dynamic performance of the overall system. The proposed controller is developed in two loops of the WECS scheme under study. The first loop is used to regulate the terminal voltage, by adjusting the self-excitation. This controller represents the reactive power control. In this case, the FLC will utilize the error and its change in terminal voltage to regulate the duty cycle of the capacitor bank. The second loop is used to adjust the mechanical power, by adapting the blade angle of WECS. Here, the FLC uses the frequency error and its change to adjust the blade angle of the wind turbine to control the active power input. The simulation results, which cover a wide range of electrical and mechanical disturbances, depict the effectiveness of the proposed controller compared with other AI techniques.

Keywords Hybrid controller · Genetic algorithm · Self-excited induction generator

A.-F. Attia (✉) · Y. A. Al-Turki
Deanship of Scientific Research, King Abdulaziz University, P.O. Box 80230,
Jeddah 21589, Saudi Arabia
E-mail: attiaa1@yahoo.com

A.-F. Attia
National Research Institute of Astronomy and Geophysics (NRIAG),
Helwan, Cairo, Egypt

Y. A. Al-Turki
Electrical and Computer Department, Faculty of Engineering,
King Abdulaziz University, Jeddah, Saudi Arabia

H. F. Soliman
Electrical Power and Machine Department, Faculty of Engineering,
Ain Shams University, Cairo, Egypt

Published online: 22 February 2012

الخلاصة

تقدم هذه الورقة متحكماً هجيناً جديداً باستخدام تقنيات الذكاء الاصطناعي لتحسين الأداء الديناميكي للمولد الحثي ذاتي الإثارة الذي يتم تحريكه عن طريق نظام تحويل طاقة الرياح. إن وسيلة الذكاء الاصطناعي تشتمل على خوارزميات جينية إضافة لمتحكم منطق مبهم، حيث إن دور هذه الخوارزميات هو الحصول على أفضل قيم لمعاملات المتحكم لضمان الأداء الأفضل للنظام الكلي. وقد تم إنجاز المتحكم المقترح في مسارين، حيث ينظم المسار الأول الجهد (الفولتية) الخارج عن طريق تعديل الإثارة الذاتية ، مما يمثل تحكما في القدرة المفاعلة ، وفي هذه الحالة يستخدم متحكم المنطق المبهم الخطأ والتغير في قيمة الجهد لتنظيم دورة الأداء للمكثفات. أما المسار الثاني فيستخدم لتعديل القوة الميكانيكية عن طريق زاوية شفرات نظام طاقة الرياح . وفي هذه الحالة يستخدم المتحكم الخطأ في الذبذبة والتغير فيها لتعديل زاوية الشفرة لتوربين الرياح ، وذلك من أجل التحكم في القوة الفعالة المدخلة. وتوضح نتائج المحاكاة التي تغطي مدى واسعا من التغيرات الكهربائية والميكانيكية فعالية المتحكم المقترح (AFLC) للنظام تحت الدراسة مقارنة بنظم الذكاء الاصطناعي الأخرى.

1 Introduction

Many publications in the field of SEIG have dealt with solutions to a range of problems (e.g., enhancing performance, loading, interfacing with the grid, etc.). El Sousy et al. [1] discussed a method for controlling a three-phase induction generator using indirect field orientation control, while Mashaly et al. [2] introduced an FLC controller for a wind energy utilization scheme. Induction generators have been widely employed to operate as wind-turbine generators and small hydroelectric generators for isolated power systems [3,4]. Induction generators can be connected to large power systems, to inject electric power, when the rotor speed of the induction generator is greater than the synchronous speed of the air-gap-revolving field. In this paper, the dynamic performance is studied for SEIG driven by WECS to feed an isolated load. The d–q axes equivalent circuit model based on different reference frames extracted from fundamental machine theory is employed to analyze the response of the machine dynamic performance [3,4]. The voltage controller for SEIG adapts the terminal voltage via a semiconductor switching system. The semiconductor switch regulates the duty cycle, which adjusts the value of the capacitor bank connected to the SEIG [5,6]. The SEIG is equipped with a frequency controller to regulate the mechanical input power. In addition, the stator frequency is regulated. This is achieved by adjusting the pitch angle of the wind turbine. In this paper, the proposed controller will be carried out in two loops for the WECS scheme under study. The first FLC will utilize the error in terminal voltage and its change to regulate the duty cycle of the capacitor bank. The second FLC uses the frequency error and its change to adjust the blade angle of the wind turbine to control the active power input. The proposed GA is used to optimize the parameters of the fuzzy sets for both FLCs to ensure a better dynamic performance of the WECS.

2 The System Under Study

Figure 1 shows the block diagram for the system under study, which consists of self-excited induction generator (SEIG) driven by WECS connected to an isolated load. There are two controller loops: one for voltage control through the reactive power controller and the second for active power control via control of the pitch angle.

The mathematical model of SEIG driven by WECS is simulated using the MATLAB/SIMULINK package to solve the differential equations. Two controllers have been developed for this system. The first ones is the voltage controller to adjust the terminal voltage. The second controller is the frequency controller to regulate the input power to keep the stator frequency constant.

3 Mathematical Model of the SEIG Driven by WECS

3.1 The Electrical Equation of the SEIG

The stator and rotor voltage equations using the Krause transformation [3,4], based on a stationary reference frame, are given in the Appendix (A) [7].

3.2 The Mechanical Equations of the WECS

The mechanical equations relating the power coefficient of the wind turbine, the tip speed ratio (μ) and the pitch angle (β) are given in Refs. [7–9]. The analysis of an SEIG in this study is performed taking the following assumptions into account [3].

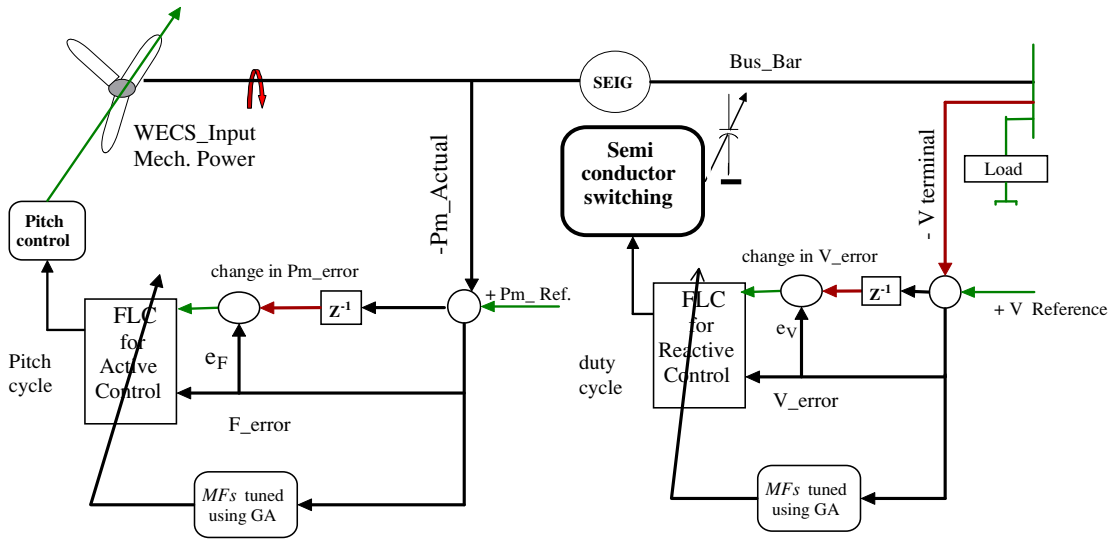

Fig. 1 System under study

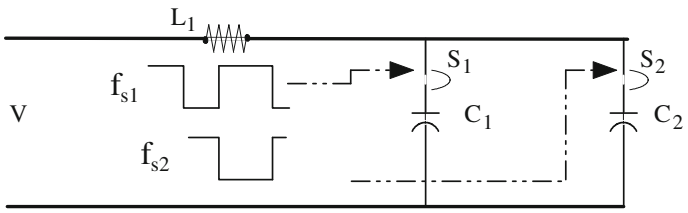

Fig. 2 Semiconductor switches (S_1, S_2) circuit for capacitor bank

3.3 Voltage Control Via Switching Capacitor Bank Technique

3.3.1 Switching

Capacitor switching has been discarded in the past because of the practical difficulties involved due to the occurrence of voltage and current transients [5,6]. It has been argued, and justly so, that current 'spikes', for example, would inevitably exceed the maximum current rating as well as the $(\mathrm{d}i/\mathrm{d}t)$ value of a particular semiconductor switch. The only way out of this dilemma would be to design the semiconductor switch to withstand the transient value at the switching instant. Meanwhile, the equivalent circuit in Fig. 2 is added to explain this situation of the switching capacitor bank due to the duty cycle. The details of this circuit are given in Ref. [6]. For the circuit shown in Fig. 2, the switches are operated in anti-phase, i.e., the switching function f_{s2} which controls switch S_2 is the inverse function of f_{s1} which controls switch S_1. In other words, switch S_2 is closed during the time when switch S_1 is open, and vice versa.

3.3.2 Voltage Control

As shown in Fig. 1, the input to controller is the voltage error, while the output of the controller is used to execute the duty cycle (λ). The value of calculated (λ) is used as an input to the semiconductor switches to change the value of the capacitor bank according to the need for the effective value of the excitation. Accordingly, the terminal voltage is controlled by adjusting the self-excitation through automatic switching of the capacitor bank.

3.3.3 Frequency Control

Frequency control is applied to the system by adjusting the pitch angle of the wind turbine blades. This is used to keep the SEIG operating at a constant stator frequency and to counteract the speed disturbance effect.

The pitch angle is a function of the power coefficient (C_p) of the wind turbine WECS. The value of (C_p) is calculated using the pitch angle value according to Eq. (12) in Appendix C. Consequently, the best adjustment for the value of the pitch angle improves the mechanical power regulation, which, in turn, achieves a better adaptation for the frequency of the overall system. Accordingly, the frequency control regulates the mechanical power of the wind turbine.

4 Controllers

Three different types of controller strategies have been conducted. First, the conventional PI controller with variable gains is applied. Second and third, FLC with static and adapted fuzzy sets using genetic algorithms are applied to adjust the value of the integral gain (K_I) for both frequency and voltage controllers.

4.1 Conventional PI-Controller with Variable Gain

Based on the mathematical model of the system, equipped with two controllers (PI & FLC) for terminal voltage and blade angle, the simulation is carried out using the MATLAB–Simulink Package as shown in Appendix D. It runs for a PI controller with varying integral gain, finding a relation between the voltage or frequency error and the value of these gains. A program has been developed to compute the value of the variable integral gain K_{IV}, as shown in Fig. 3, using the following rule [11].

$$
\begin{aligned}
&\text{if } (e_V < e_{V\,\min})\\
&\quad K_{IV} = K_{IV\,\min};\\
&\text{elseif } (e_V > e_{V\,\max}),\\
&\quad K_{IV} = K_{IV\,\max};\\
&\text{else } (e_{V\,\min} < e_V < e_{V\,\max}),\\
&\quad M = (K_{IV\,\max} - K_{IV\,\min})/(e_{V\,\max} - e_{V\,\min});\\
&\quad C = K_{IV\,\min} - M \times e_{V\,\min};\\
&\quad K_{IV} = (M \times e_V) + C;\\
&\text{end}
\end{aligned}
$$

where, e_V is the voltage error, $e_{V\,\min}$ the minimum value of the voltage error, $e_{V\,\max}$ the maximum value of the voltage error, $K_{IV\,\min}$ the minimum value of the integral gain in the V/Q control loop (K_{IV}), $K_{IV\,\max}$ the maximum value of the integral gain in the V/Q control loop (K_{IV}), C is a constant and M is the slope K_{IV} curve. Figure 3 shows the rule for calculating K_{IV} in accordance with the terminal voltage error e_V. The value

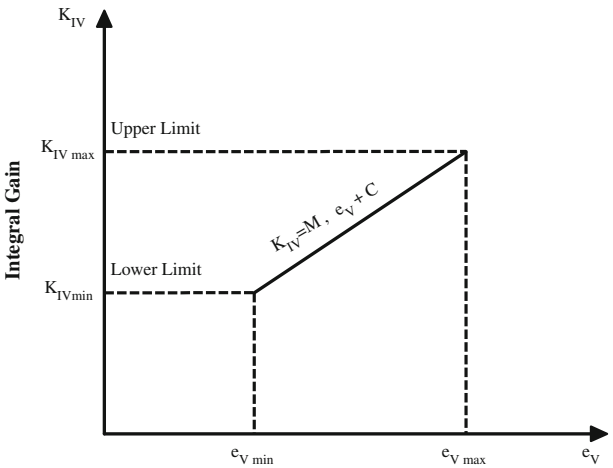

Fig. 3 Variable integral gain for PI controller

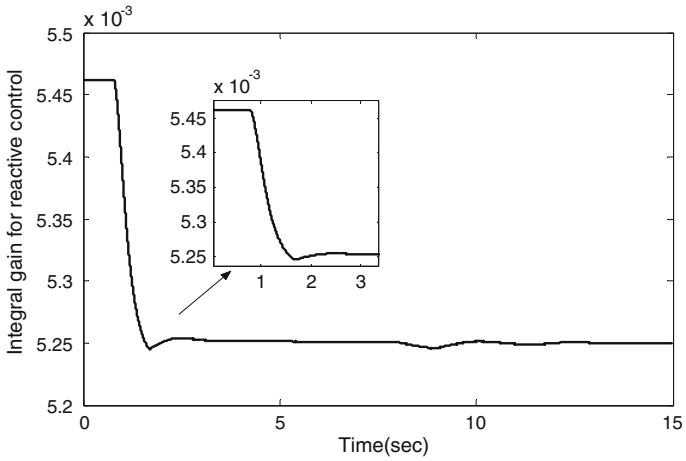

Fig. 4 Variable integral gain in PI-voltage controller with FLC

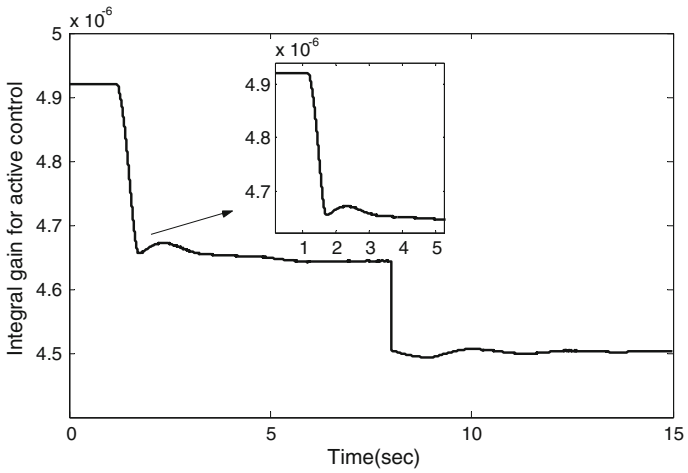

Fig. 5 Variable integral gain in PI-frequency controller with FLC

of $e_{\mathrm{V\,min}}$ and $e_{\mathrm{V\,max}}$ is obtained by trial and error to give the best dynamic performance. The proportional gains (K_{PV} and K_{PF}) are also kept constant for the voltage and frequency controllers, respectively. Various characteristics are tested to study the effect of changing the value of (K_{IV}) to update the voltage control. The simulation results cover the starting period and the period when the system is subjected to a sudden increase in the load, at instant 8 s. Figures 4 and 5 show the effect of variable voltage integral gain K_{IV} and frequency K_{IF} controllers versus time, respectively.

4.2 The Fuzzy Logic Controller

To design the fuzzy logic controller, the control engineer must gather information on how the artificial decision maker should act in the closed-loop system, and this would be done from the knowledge base [10]. The fuzzy system is constructed from input fuzzy sets, fuzzy rules and output fuzzy sets, based on the prior knowledge base of the system. Figure 6 shows the basic construction of the FLC with the system under study. There are rules, in FLC, to govern and execute the relations between inputs and outputs of the system. Every input and output parameter, in FLC, has a membership function, which could be introduced between the limits of these parameters through a universe of discourse. The FLC is used to compute and adapt the value of the variable integral gain K_{I} of PI controllers.

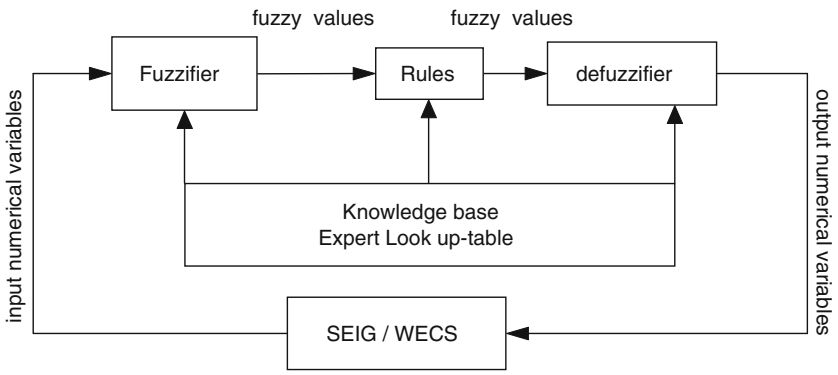

Fig. 6 The three stages of the fuzzy logic controller

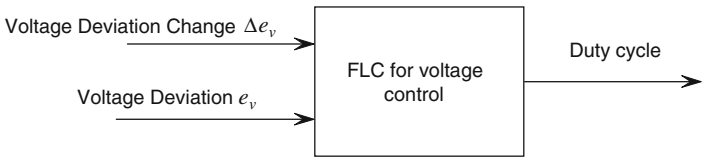

Fig. 7 Fuzzy controller for reactive control

4.2.1 Global Input and Output Variables

In the voltage/reactive power (V/Q) control, the input variables are terminal voltage deviation e_V and the change of terminal voltage deviation Δe_V. Figure 7 depicts the simplified block diagram of the FLC and the related input and output variables used in V/Q controller. Five linguistic variables are used for each of the input variables, as shown in Fig. 8a, b, respectively. The output variable fuzzy set, which represents the value of the integral gain in the Q/V control loop K_{IV}, is shown in Fig. 8c, while Fig. 8d shows the fuzzy surface for rules.

In the frequency/active power (f/P) control, the input variables are mechanical power deviation e_F and the change of the mechanical power deviation Δe_F. Figure 9 depicts the simplified block diagram of the FLC and the related input and output variables used in V/Q controller. The output variable of this FLC is the value of the integral gain (K_{IV}) in the f/P control loop.

Five linguistic variables are used for each of the input variables, as shown in Fig. 10a, b, respectively. The output variable fuzzy set is shown in Fig. 10c, while Fig. 10d shows the fuzzy surface. The linguistic variables have been used for the input variables, as shown in Fig. 10a, b, c, are P for Positive, N for Negative, AV for Average, B for Big and S for Small. The combinations of these linguistic variables are used, for example, PB is Positive Big and NS is Negative Small, etc. After constructing the fuzzy sets for input and output variables, it is required to develop the set of rules, the so-called look-up table, which defines the relation between the input variables, e_V, e_F, Δe_V and Δe_F and the related output variable of the fuzzy logic controller. Table 1 depicts the look-up table of the fuzzy set rules for V/Q control loop. Meanwhile, Table 2 shows the look-up table of the fuzzy set rules for f/P control loop.

4.2.2 The Defuzzification Method

The minimum of maximum method has been used to find the output fuzzy rules representing a polyhedron map, as shown in Fig. 11. First, the minimum membership grade is calculated from the minimum value for the intersection of the two input variables (e_V and Δe_V) with the related fuzzy set in that rule. This minimum membership grade is calculated to rescale the output rule, and then the maximum is taken, as shown in Fig. 11. Finally, the centroid or center of area is used to compute the fuzzy output, which represents the defuzzification stage, as follows [10]:

$$K_I = \frac{\int y\mu(y)\,\mathrm{d}y}{\int \mu(y)\mathrm{d}y} \tag{1}$$

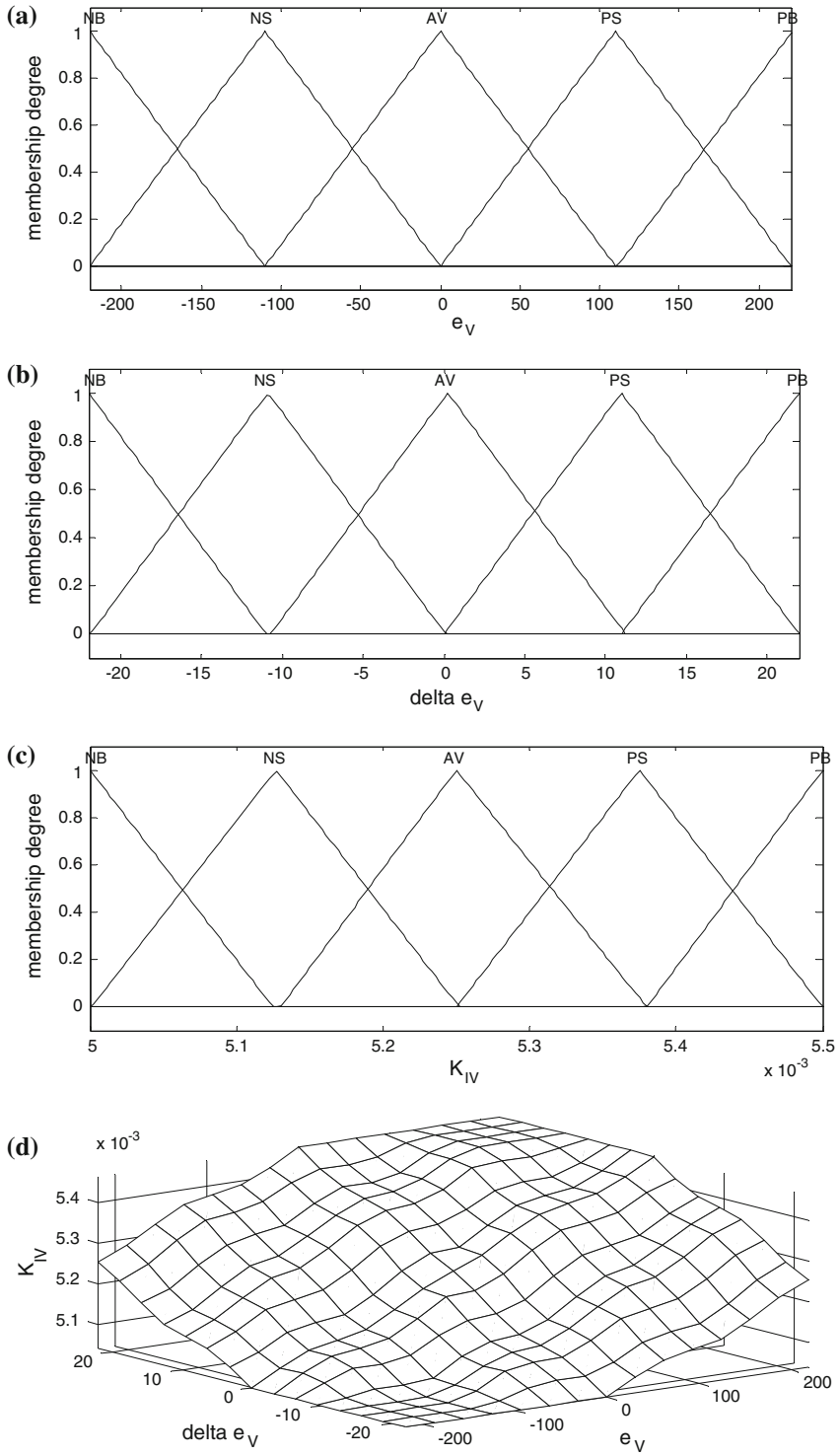

Fig. 8 **a** Membership functions of voltage error, **b** membership functions of change in voltage error, **c** membership functions of the integral gain in the Q/V control loop (K_{IV}), **d** fuzzy surface for rules

5 Genetic Algorithm for Optimizing Fuzzy Controllers

The adaptive fuzzy logic controller (AFLC), using adaptive fuzzy set, has the same inputs and output as the static fuzzy logic controller (SFLC). The SFLC is defined as an FLC using a fixed structure of fuzzy set. A

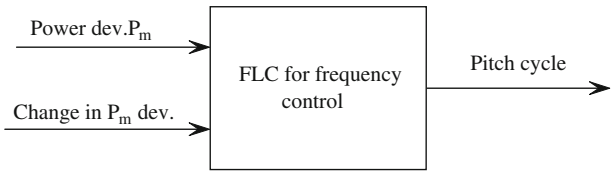

Fig. 9 Fuzzy controller for active control

full rule base has 25 rules. The rules have the general form:

$$\text{If Vector } (x_1) \text{ is NS and Change in Vector } (x_2) \text{ is AV then Output}(Y) \text{ is NS.}$$

where the membership function (mf_i) is defined as follows:
$\text{mf}_j \in \{NB, NS, AV, PS \text{ and } PB\}$ as in the static fuzzy case. However, the output space has five different fuzzy sets. To accommodate for the change in operating conditions, the adaptation algorithm changes the parameters of the inputs and output fuzzy sets.

The algorithm presented in this section is designed to optimize a rule base of the fuzzy controller by shifting and/or modifying the support of the input fuzzy sets. They do not modify the rules or the structure of the fuzzy controller. The fuzzy sets $\mu_j^{(i)}$ representing the linguistic variable will be considered as a triangular membership function for the input and output variables, respectively, as shown in Fig. 12. Meanwhile, it could be defined by the following equations:

$$\mu_j^{(i)}(x) \stackrel{\text{def}}{=} \begin{cases} \frac{x - a_j^{(i)}}{b_j^{(i)} - a_j^{(i)}} & \text{if } x \in [a_j^{(i)}, b_j^{(i)}], \\ \frac{c_j^{(i)} - x}{b_j^{(i)} - a_j^{(i)}} & \text{if } x \in [b_j^{(i)}, c_j^{(i)}], \\ 0 & \text{otherwise,} \end{cases} \tag{2}$$

where $a_j^{(i)}, b_j^{(i)}, c_j^{(i)} \in \Re, a_j^{(i)} \le b_j^{(i)} \le c_j^{(i)}$; $a, b,$ and c are constant, and $\Re$ is the real integer number set. This means that $\mu_j^{(i)}(a_j^{(i)}) = 0, \mu_j^{(i)}(b_j^{(i)}) = 1,$ and $\mu_j^{(i)}(c_j^{(i)}) = 0$. The triangular membership functions will be used as symmetric fuzzy sets in the consequents and antecedents [12].

The membership function parameters of the FLCs are optimized based on genetic algorithm (GA). GA is used to calculate the optimum value of the fuzzy set parameters based on the best dynamic performance and domain search of the parameters. The objective function used in the GA technique is $(F = 1/(1 + J))$, where (J) is the minimum cost function; this will be defined later. The GA uses its operators and functions to find the values of fuzzy set parameters of the FL controllers to achieve a better dynamic performance of the overall system. These values of parameters lead to the optimum value of control actions for which the system reaches the desired values, while improving percentage of overshoot (P.O.S), rising time and oscillations.

The main aspect of GA approach is to optimize the fuzzy set parameters of FL controllers as used in [13]. The flowchart procedure for the GA optimization process is shown in Fig. 13.

5.1 Representation of Fuzzy Set Parameters in GA

The fuzzy set parameters of FL controllers are formulated using the GA approach and are represented in a chromosome. The chromosome representation determines the GA structure. The fuzzy set parameters of FL controllers are initially started using values of static fuzzy set parameters. The minimum performance criteria J are [2]:

$$J = \int_0^T (\alpha_1 |e(t)| + \beta_1 |e'(t)| + \gamma_1 |e''(t)|)\, \mathrm{d}t \tag{3}$$

where $e(t)$ is equal to e_V or e_F. The parameters (α_1, β_1 and γ_1) are weighting coefficients.

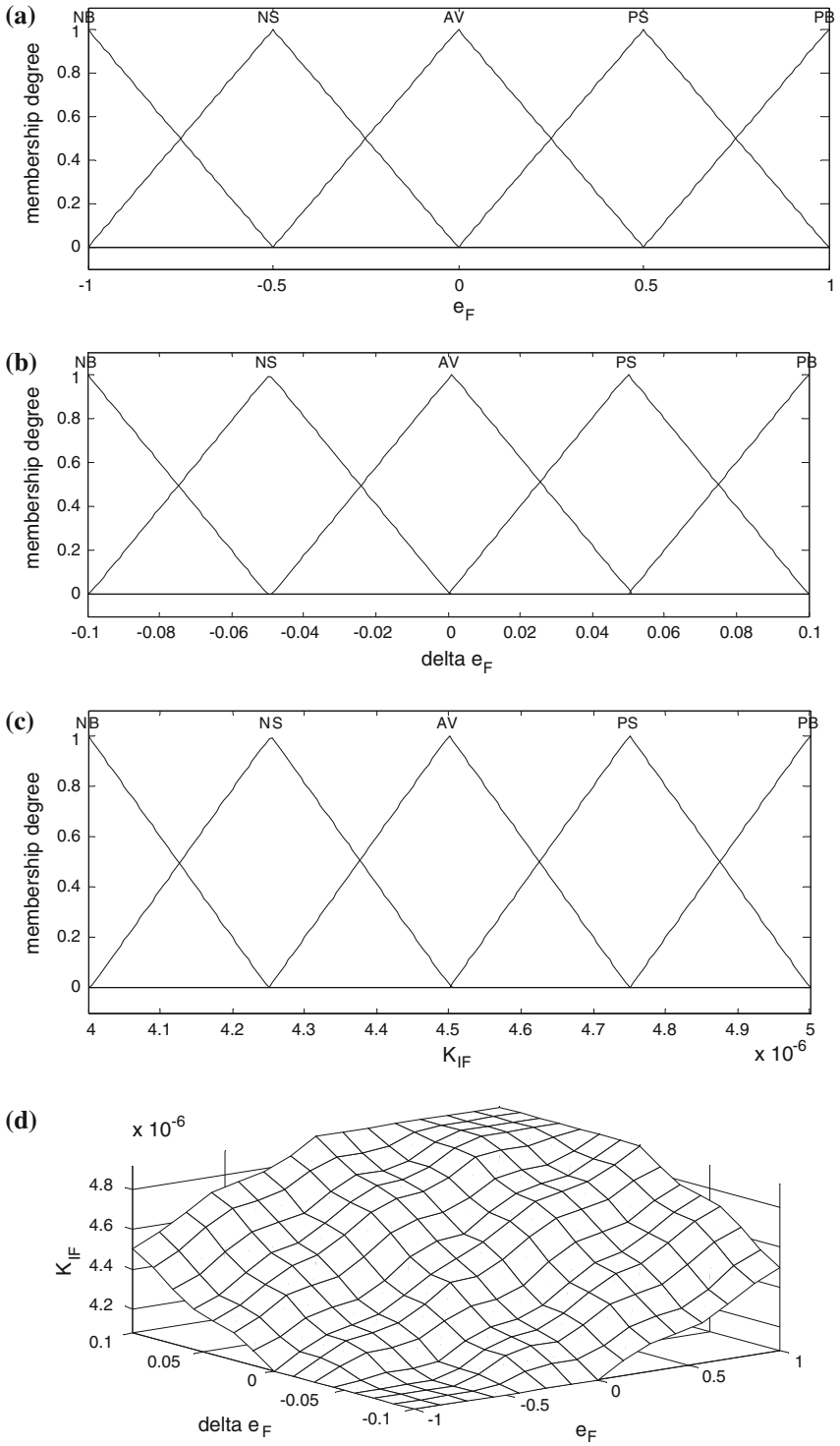

Fig. 10 **a** Membership functions of mechanical power error, **b** membership functions of change on mech. power error, **c** membership functions of variable K_{IF}, **d** fuzzy surface for rules

5.2 Coding of Fuzzy Set Parameters

The coded parameters are arranged on the basis of their constraints to form a chromosome of the population. The binary representation is the coded form for parameters with chromosome length equal to the sum of bits for

Table 1 Look-up table of fuzzy set rules for voltage control

Voltage deviation (e_V)	Voltage deviation change (Δe_V)				
	NB	NS	AV	PS	PB
NB	NB	NB	NB	NS	AV
NS	NB	NB	NS	AV	PS
AV	NB	NS	AV	PS	PB
PS	NS	AV	PS	PB	PB
PB	AV	PS	PB	PB	PB

Table 2 Look-up table of the fuzzy set rules for f/P control

Mechanical power deviation (e_F)	Change of the mechanical power deviation (Δe_F)				
	NB	NS	AV	PS	PB
NB	NB	NB	NB	NS	AV
NS	NB	NB	NS	AV	PS
AV	NB	NS	AV	PS	PB
PS	NS	AV	PS	PB	PB
PB	AV	PS	PB	PB	PB

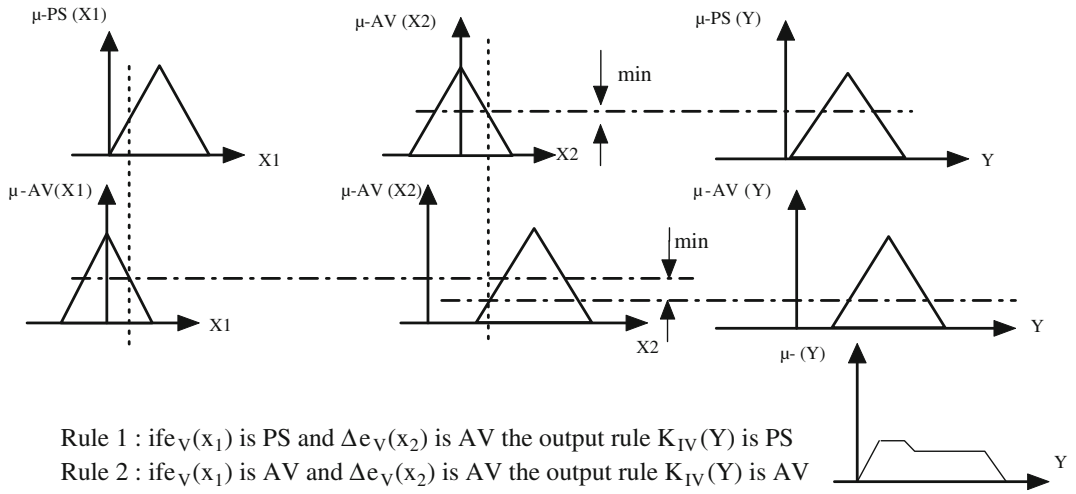

Fig. 11 Schematic diagram of the defuzzification method using the center of area

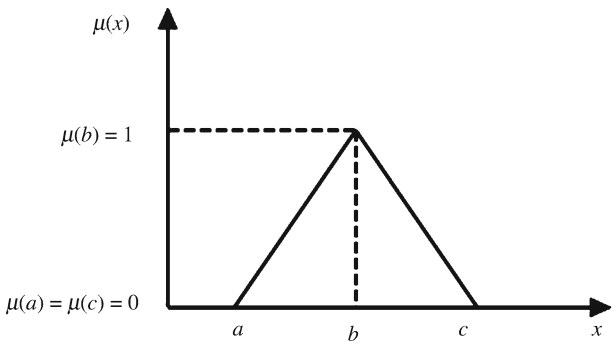

Fig. 12 Triangular membership function (*MF*)

all parameters. Figures 14 and 15 show the coded parameters of FLCs for reactive and active power controllers, respectively. The chromosome length used in this paper was 900 bits, where the bit length of each parameter equals 10 bits.

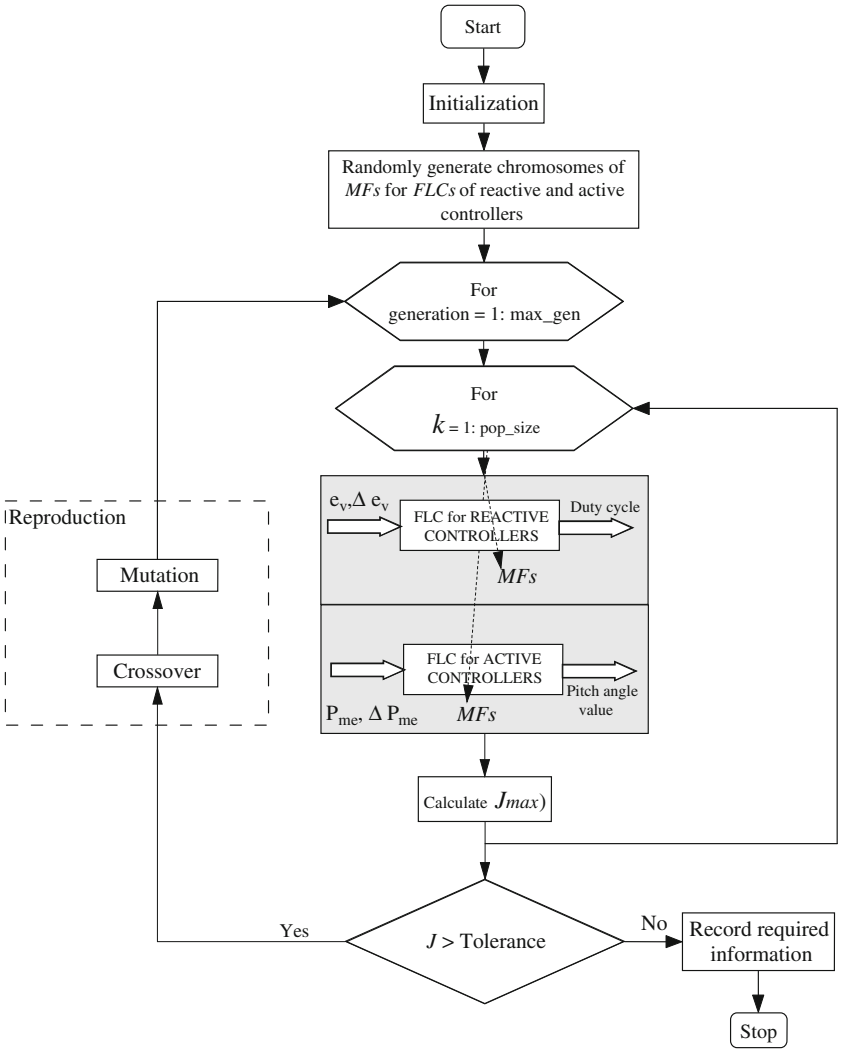

Fig. 13 Flowchart of GA approach for optimizing *MFs*

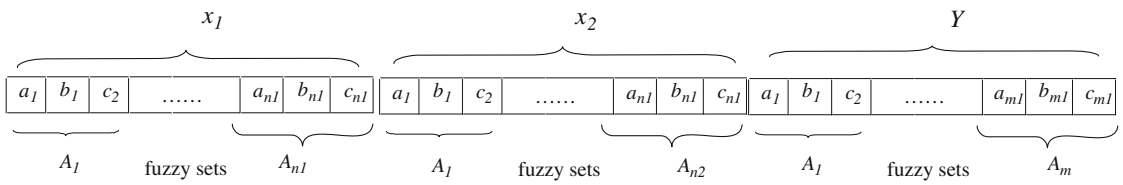

Fig. 14 Coded parameters of FLC for reactive power controller

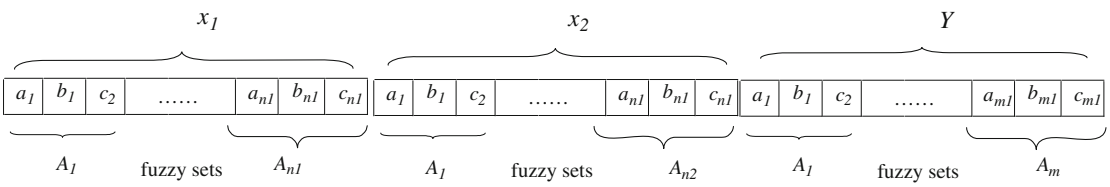

Fig. 15 Coded parameters of FLC for active power controller

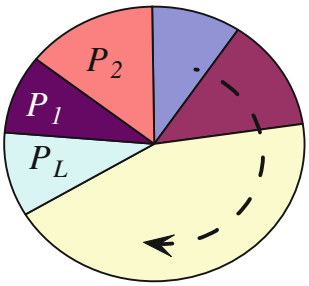

Fig. 16 Roulette wheel selection scheme

5.3 Selection Function

The selection strategy decides how to select individuals to be parents for new 'children'. The selection usually applies some selection pressure by favoring individuals with better fitness. After procreation, the suitable population consists, for example, of L chromosomes, which are all initially randomized. Each chromosome has been evaluated and associated with fitness, and the current population undergoes the reproduction process to create the next population as shown in Fig. 16. The chance on the roulette wheel is adaptive and given as $P_l / \sum P_l$, as in Eq. (4) [8]:

$$P_l = \frac{1}{J_l}, \quad l \in \{1, \ldots, L\} \tag{4}$$

where J_l is the model performance encoded in the chromosome measured in the terms used in Eq. (3).

Maximizing the fitness function of each chromosome, which is inversely proportional to the performance criteria, Eq. (3) will damp the overshoot or the oscillations [8].

5.4 Crossover and Mutation Operators

The mating pool is formed, and crossover is applied. Then, mutation operation is applied followed by GA approach. Finally, after these three operations, the overall fitness of the population is improved. The procedure is repeated until termination condition is reached. The termination condition is the maximum allowable number of generations, or reading a certain value of J. This procedure is shown in the flowchart given in Fig. 13.

6 Simulation Results and Discussions

6.1 Dynamic Performance Due to Sudden Load Variation

Based on system model, equipped with three controllers, PI, SFLC and AFLC for terminal voltage and blade angle, the simulation is carried out using MATLAB–Simulink Package. The simulation program uses fuzzy set for input and output variables, for both controllers V/Q and f/P, as shown in Figs. 8 and 10. It can be noticed that terminal voltage error (e_{V}) varies between -220 and 220 and its change (Δe_{V}) varies between -22 and 22. The output of FLC is K_{IV}, which changes between 5e$-$003 and 5.5e$-$003. From Fig. 10, it can be noticed that the mechanical power error (e_{F}) varies between -1 and 1 and its change (Δe_{F}) varies between -0.1 and 0.1. The output of FLC is K_{IF}, which changes between 4e$-$006 and 5e$-$006. Figure 12 depicts the result when the system is initially loaded by an impedance having $R = 40$ ohm and $L = 0.12$ H; later, the load is changed to 80 ohm and 0.12 H. Figure 18 depicts system response sudden change in load at time = 10 s. Figures 17 and 18 show the simulation results for the system under study equipped with a conventional controller (PIC) having variable integral gain, static FLC and the AFLC algorithms. The proposed static and adapted FLCs are used to adapt K_{I} to give a better dynamic performance for the overall system, as shown in Figs. 17 and 18, regarding P.O.S and settling time compared with PI with variable K_{I} for different

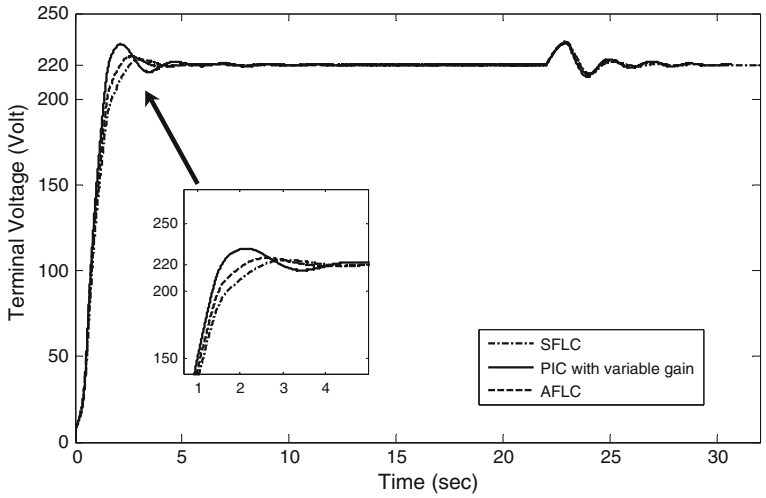

Fig. 17 Dynamic response of terminal voltage for PIC, SFLC and AFLC

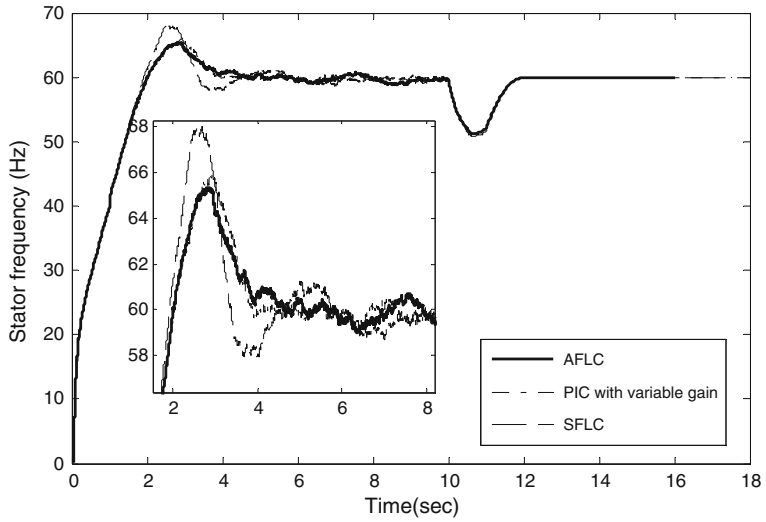

Fig. 18 Dynamic response of stator frequency for PIC, SFLC and AFLC

loads. Figures 19 and 20 depict the simulation results for the controller's duty cycle and the load current, respectively.

6.2 Dynamic Performance Due to Sudden Wind Speed Variation

The dynamic performance of the overall system is investigated of the overall system when it is subjected to a sudden disturbance of wind speed from 7 to 15 m/s. Figures 21 and 22 show the simulation results of wind speed variation and the stator frequency, respectively. These Figs. 21 and 22 show the ability of the proposed AFLC controller to overcome the speed variation as well the SFLC and PIC with variable integral gain.

7 Conclusion

This paper introduced a novel application of hybrid controller using artificial intelligence (AI) techniques to improve the dynamic performance of the self-excited induction generator "SEIG" driven by wind energy conversion scheme "WECS". The proposed AFLC is applied to frequency and voltage controls of the system to enhance its dynamic performance. AFLC is used to regulate the duty cycle of the switched capacitor bank to

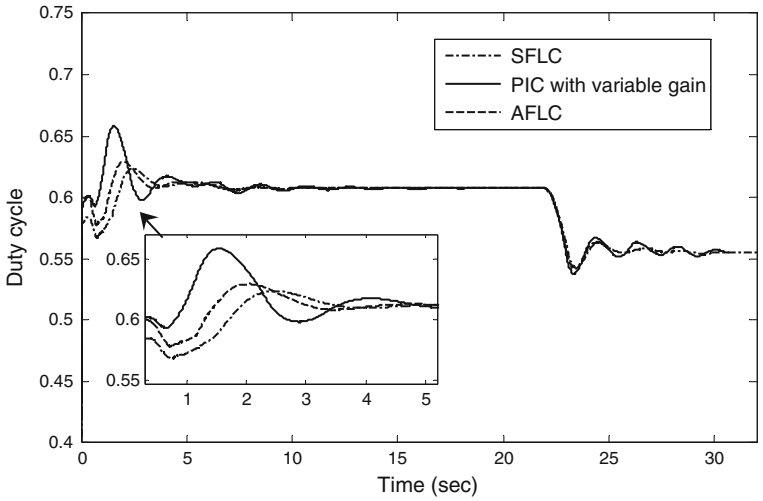

Fig. 19 Dynamic response of duty cycle for PIC, SFLC and AFLC controllers

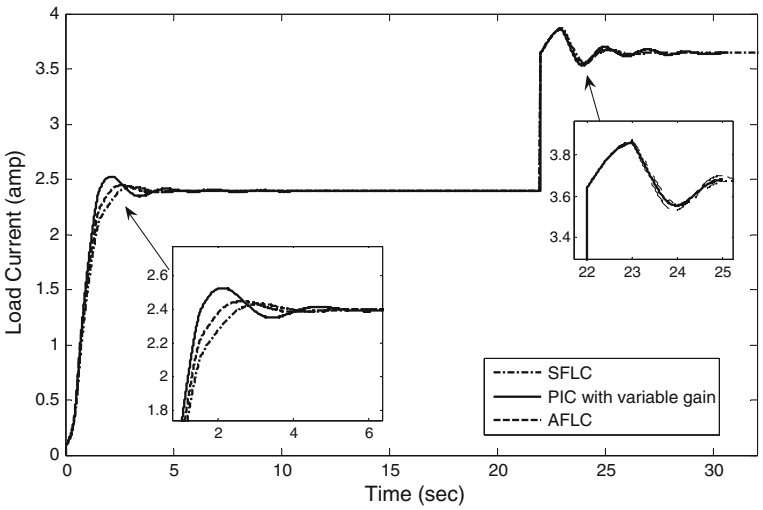

Fig. 20 Dynamic response of load current for PIC, SFLC and AFLC controllers

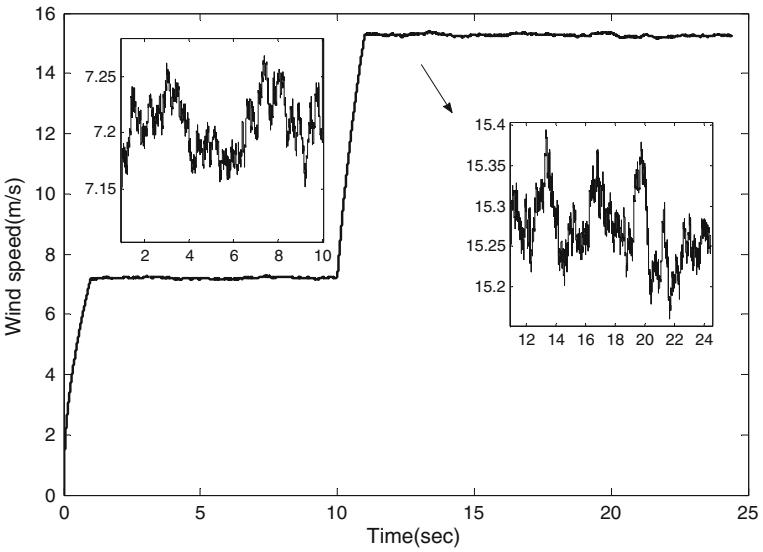

Fig. 21 Sudden variation of wind speed versus time

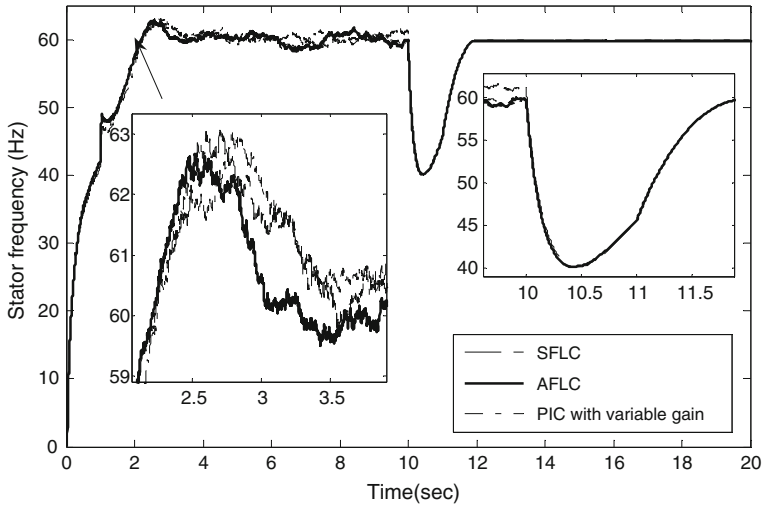

Fig. 22 Stator frequency according to wind speed variation for SEIG controlled by SFLC, AFLC and PIC controllers

adjust the terminal voltage of the induction generator. AFLC is also applied to regulate the blade angle of the wind energy turbine to control the stator frequency. The simulation results show better dynamic performance of the overall system using the AFLC controller than for the variable PI type and SFLC. Another simulation has been conducted to study system dynamic performance following a sudden wind speed variation. A classical fuzzy logic controller, using a fixed fuzzy set, was simulated and tested. Simulation results show the superiority of the adaptive fuzzy controller over other controllers.

Acknowledgments The authors acknowledge the Deanship of Scientific Research, King Abdulaziz University, for supporting project No. 4-021-429 and encouragement throughout the study.

Appendix (A): SEIG Differential Equation

v_{ds} "Stator Voltage 's (volt) Differential Equation in Direct Axis"

$$v_{ds} = -R_s.i_{ds} - \left(\frac{\omega}{\omega_b}\right) \times (-x_{ls}.i_{qs} + x_m(i_{qr} - i_{qs})) + p\left(\frac{-x_{ls}.\, i_{ds} + x_m(i_{dr} - i_{ds})}{\omega_b}\right) \tag{5}$$

v_{qs} "Stator Voltage 's Differential Equation at Quadrate Axis"

$$v_{qs} = -R_s.i_{qs} + \left(\frac{\omega}{\omega_b}\right)(-x_{ls}.i_{ds} + x_m(i_{dr} - i_{ds})) + p\left(\frac{(-x_{ls}.i_{qs} + x_m(i_{qr} - i_{qs}))}{\omega_b}\right) \tag{6}$$

v_{dr} "Rotor Voltage 's Differential Equation in Direct Axis"

$$v_{dr} = R_r.i_{dr} - \left(\frac{(\omega - \omega_r)}{\omega_b}\right) x_{lr}.i_{qr} + x_m(i_{qr} - i_{qs}) + p\left(\frac{(x_{lr}.i_{dr} + x_m(i_{dr} - i_{ds}))}{\omega_b}\right) \tag{7}$$

v_{qr} "Rotor Voltage 's Differential Equation in Quadrate Axis"

$$v_{qr} = R_r.i_{qr} + \left(\frac{(\omega - \omega_r)}{\omega_b}\right) x_{lr}.i_{dr} + x_m(i_{dr} - i_{ds}) + p\left(\frac{(x_{lr}.i_{qr} + x_m(i_{qr} - i_{qs}))}{\omega_b}\right) \tag{8}$$

Flux Linkage Differential Equation for Stator and Rotor components:

$$\varphi_{ds} = -x_{ls}.i_{ds} + x_m(i_{dr} - i_{ds}) \tag{9}$$

where φ_{ds} is the stator flux linkage (Weber) in direct axis and i_{dr} is the rotor current (amp) in direct axis, but i_{ds} is the stator current (amp) in direct axis and p is operator = d/dt

$$\varphi_{qs} = -x_{ls}.i_{qs} + x_m(i_{qr} - i_{qs}) \tag{10}$$

where φ_{qs} is the stator flux linkage in quadrant axis and i_{qr} is the rotor current in quadrant axis, but i_{qs} is the stator current in quadrant axis

$$\varphi_{dr} = X_{lr}.i_{dr} + X_m(i_{dr} - i_{ds}) \tag{11}$$

where φ_{dr} is the rotor flux linkage in direct axis

$$\varphi_{qr} = x_{lr}.i_{qr} + x_m(i_{qr} - i_{qs}) \tag{12}$$

where φ_{qr} is the rotor flux linkage in quadrant axis v

$$\frac{d\varphi_{qs}}{dt} = \omega_b.(V_{qs} + R_s i_{qs} - \varphi_{ds}) \tag{13}$$

where ω_b is the base speed
Magnetizing reactance equation:

$$x_m = \begin{cases} 105.77 & \text{at } 0.0 \le i_m < 0.864 \\ (340.2)/(i_m + 2.35) & \text{at } 0.864 \le i_m < 1.051 \\ (227.4)/(i_m + 1.22) & \text{at } 1.051 \le i_m < 1.476 \\ (202.3)/(i_m + 9.3) & \text{at } 1.476 \le i_m < 1.717 \\ (179.8)/(i_m + 6.3) & \text{at } 1.717 \le i_m \end{cases} \tag{14}$$

Appendix (B): SEIG Parameters

The induction machine under study as an SEIG is a three-phase (1.1 kW, 127/220 V (line voltage), 8.3/4.8 A (line current), 60 Hz, 2 poles), wound-rotor induction machine [9,10]. By choosing proper base values:

base voltage (V_b) = [220/(1.73)]V,
base current (I_b) = 4.8A,
base impedance (Z_b) = 26.462 ohm,
base rotor speed (N_b) = 3,600 rpm, and
base frequency (F_b) = 60 Hz.
The per-unit parameters of the induction machine under study are equal:
stator resistance (Rs) = 0.0779 Ω,
rotor resistance (R_r) = 0.0781 Ω,
stator reactance (x_s) and rotor reactance (x_r) are equal to 0.0895 Ω.

The equation of motion of rotating parts of the combined studied SEIG and the wind turbine is also included in the system for having a detailed simulation model. The inertia constant of the machine (H) is 0.055 s.

Appendix (C): Mechanical Differential Equations

$$P_m = \left(\frac{1}{8}\right)(\pi \rho C_p D^2 V_w^3) \tag{15}$$

$$\omega_m = (2\pi n)/60 \tag{16}$$

$$T_m = \left(P_m/\omega_m\right) \tag{17}$$

$$C_p = \left[(0.44 - 0.0167\beta).\sin\left(\frac{\pi(\mu - 3)}{(15 - 0.3 \times \beta)}\right) - 0.00184(\mu - 3)\beta\right] \tag{18}$$

$$\mu = \omega_m\left(\frac{R}{V_w}\right) = \left(\frac{D\pi n}{60 \times V_w}\right) \tag{19}$$

$$\frac{d\omega_r}{dt} = \left(\frac{\omega_b}{2H}\right)(T_m - T_e - B_a.\omega_r) \tag{20}$$

where:

ω_m: the mechanical speed (rad/s),
P_m: the mechanical power (KW),
T_m: the mechanical torque (nm),
n: is the rotor revolution per minute (rpm),

C_p: the power coefficient of the wind turbine,
β: the blade pitch angle (°),
μ: is the tip speed ratio,
V_w : the wind speed (m/s),
R: the rotor radius (m) of the wind turbine,
D: the rotor diameter (m) of the wind turbine,
B_a: the friction factor,
T_e: the electrical torque (nm) and $\pi = 3.14$ and ρ = air density (Kg/m^3), where: ω_r is the rotor speed (rad/s).

Appendix (D): Simulation Block Diagram for SEIG / WECS and its Controllers

See Figs. 23 and 24

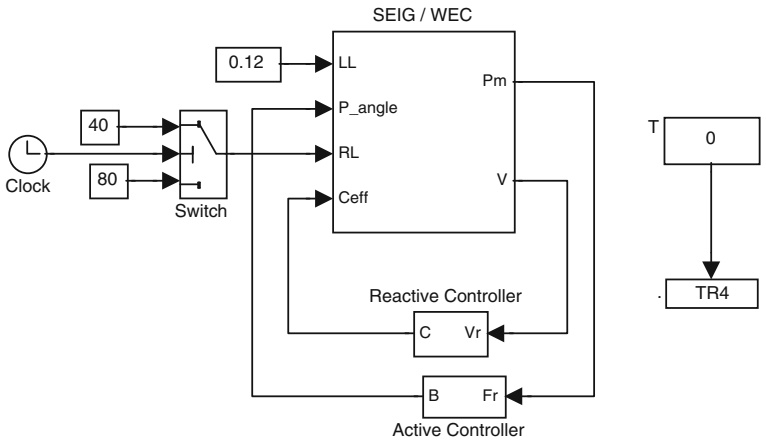

Fig. 23 Total SEIG block diagram

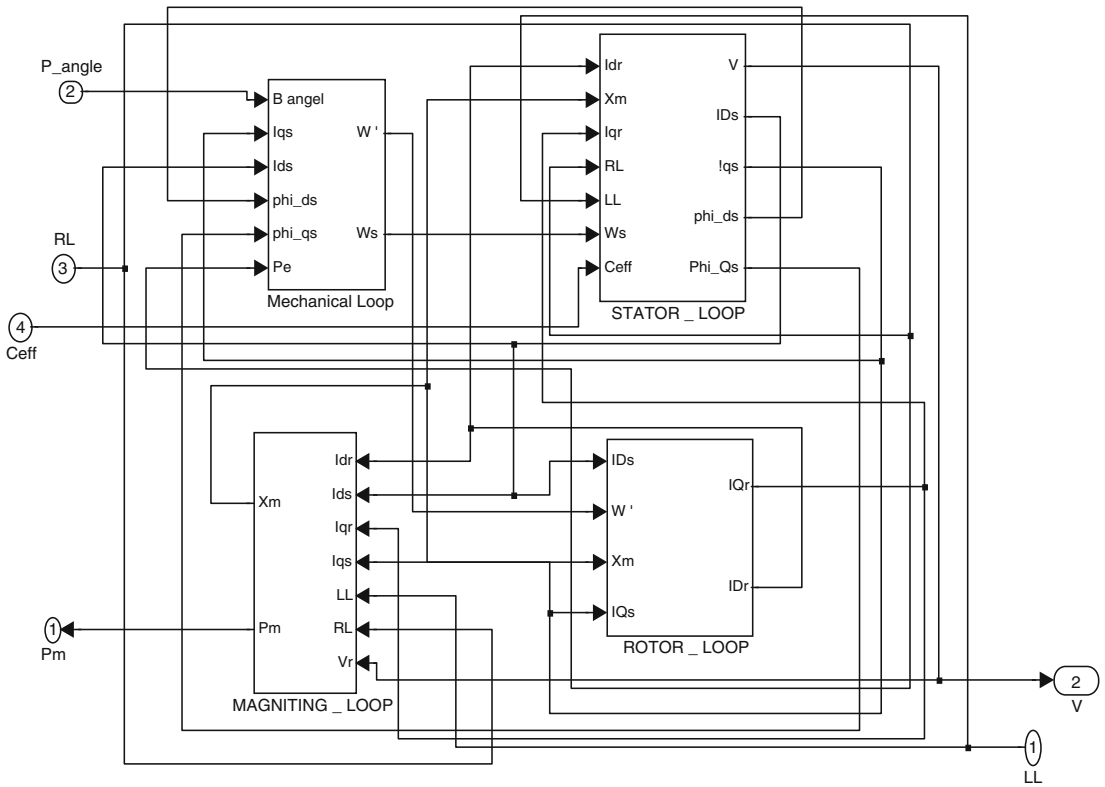

Fig. 24 Electrical and mechanical system block diagram

References

1. El-Sousy, F.; Orabi, M.; Godah, H.: Indirect field orientation control of self-excited induction generator for wind energy conversion. In: ICIT, December 2004
2. Mashaly, A.; Sharaf, M.; Mansour, M.; Abd-Satar, A.A.: A fuzzy logic controller for wind energy utilization scheme. In: Proceedings of the 3rd IEEE Conference of Control Application. 24–26 August 1994, Glasgow, Scotland, UK
3. Li, W.; Yi-Su, J.: Dynamic performance of an isolated self excited induction generator under various loading conditions. IEEE Trans. Energy Convers. **15**(1), 93–100 (1999)
4. Li, W.; Ching-Huei, L.: Long-shunt and short-shunt connections on dynamic performance of a SEIG feeding an induction motor load. IEEE Trans. Energy Convers. **14**(1), 1–7 (2000)
5. Atallah, A.M.; Adel, A.: Terminal voltage control of self excited induction generators. In: Sixth Middle-East Power Systems Conference MEPCON'98. Mansoura, Egypt, 15–17 December 1998, pp. 110–118
6. Marduchus, C.: Switched capacitor circuits for reactive power generation. Ph.D. Thesis, Brunuel University (1983)
7. Soliman, H.F.; Attia, A.F.; Mokhymar, S.M.; Badr, M.A.L.; Ahmed, A.E.M.S.: Dynamic Performance Enhancement of Self Excited Induction Generator Driven by Wind Energy Using ANN Controllers. Sci. Bull. Fac. Eng. Ain Shams Univ. Part II. **39**(2), pp. 631–651 (2004)
8. Mokhymar, S.M.: Enhancement of the performance of wind driven induction generators using artificial intelligence control. Ph.D. thesis. Faculty of Engineering. Ain Shams University, 10 March 2005
9. Ezzeldin, S.A.; Xu, W.: Control design and dynamic performance analysis of a wind turbine-induction generator unit. IEEE Trans. Energy Convers. **15**(1), 91–96 (2000)
10. Passino, K.M.; Yurkovich, S.: Fuzzy control, library of congress cataloging-in-publication data. (Includes bibliographical references and index). Addison Wesley Longman, Inc., California. ISBN 0-201-18074-X (1998)
11. Soliman, H.F.; Attia, A.F.; Mokhymar, S.M.; Badr, M.A.L.: Fuzzy algorithm for supervisory voltage/frequency control of a self excited induction generator. Acta Polytech. **46**(6), 36–48 (2006)
12. Attia, A.F.: Adapted fuzzy controller for astronomical telescope tracking. J. Exp. Astron. Springer Neth. **18**(1), 93–108 (2006)
13. Attia, A.F.; Abdel-Hamid, R.; Quassim, M.: Prediction of solar activity based on neuro-fuzzy modeling. J. Sol. Phys. **227**(1), 177–191 (2005)